Inorg. Chem. **2003**, *42*, 457–462

Hydrothermal Preparation, Structures, and NLO Properties of the Rare Earth Molybdenyl Iodates, $RE(MoO_2)(IO_3)_4(OH)$ [RE = Nd, Sm, Eu]

Thomas C. Shehee,[†] Richard E. Sykora,[†] Kang M. Ok,[‡] P. Shiv Halasyamani,[‡] and Thomas E. Albrecht-Schmitt*,[†]

Department of Chemistry, Auburn University, Auburn, Alabama 36849, and Department of Chemistry, University of Houston, Houston, Texas 77204-5003

Received August 30, 2002

The reactions of $RE(IO_3)_3$ [RE = Nd, Sm, Eu] with I_2O_5 and MoO_3 in a 1:2:2 molar ratio at 200 °C in aqueous media provide access to $RE(MoO_2)(IO_3)_4(OH)$ [RE = Nd (**1**), Sm (**2**), Eu (**3**)] as pure phases as determined from powder X-ray diffraction data. Single crystal X-ray diffraction experiments demonstrate that these compounds are isostructural and crystallize in the chiral and polar space group $P2_1$. The structures are composed of three-dimensional networks formed from eight-coordinate, square antiprismatic RE^{3+} cations and $MoO_2(OH)^+$ moieties that are bound by bridging iodate anions. The Mo(VI) centers are present in distorted octahedral environments composed of two *cis*-oxo atoms, a hydroxo group, and three bridging iodate anions arranged in a *fac* geometry. There are four crystallographically unique iodate anions in the structures of **1**–**3**, one of these is actually present in the form of a IO_{3+1} polyhedron where a short interaction of 2.285(4) Å is formed between the iodate anion and the hydroxo group bound to the Mo(VI) center. This interaction results in significant distortions of the iodate anion similar to those found in tellurites with TeO_{3+1} units. Two of the four iodate anions are aligned along the polar *b*-axis, imparting the required polarity to these compounds. Second-harmonic generation (SHG) measurements on sieved powders of **1** show a response of 350× α-quartz. Crystallographic data: **1**, monoclinic, space group $P2_1$, a = 6.9383(5) Å, b = 14.0279(9) Å, c = 7.0397(5) Å, β = 114.890(1)°, Z = 2; **2**, monoclinic, space group $P2_1$, a = 6.9243(6) Å, b = 13.963(1) Å, c = 7.0229(6) Å, β = 114.681(1)°, Z = 2; **3**, monoclinic, space group $P2_1$, a = 6.9169(6) Å, b = 13.943(1) Å, c = 7.0170(6) Å, β = 114.542(1)°, Z = 2.

Introduction

The development of new noncentrosymmetric (NCS) materials for applications in nonlinear optical and ferroelectric devices is currently being addressed by several independent approaches including the design of multilayered films of aligned polar organic molecules,[1−3] the crystal engineering of coordination polymers,[4−6] and the preparation of phases with cooperative second-order Jahn−Teller distortions (SOJT).[7−13] The latter scheme often makes use of high-valent transition metals that are susceptible to SOJT distortions from idealized octahedral symmetry.[14−22] A classic

* To whom correspondence should be addressed. E-mail: albreth@auburn.edu.
[†] Auburn University.
[‡] University of Houston.

(1) Lin, W.; Lin, W.; Wong, G. K.; Marks, T. J. *J. Am. Chem. Soc.* **1996**, *118*, 8034.
(2) Lin, W.; Lee, T.-L.; Lyman, P. F.; Lee, J.; Bedzyk, M. J.; Marks, T. J. *J. Am. Chem. Soc.* **1997**, *119*, 2205.
(3) van der Boom, M. E.; Richter, A. G.; Malinsky, J. E.; Lee, P. A.; Armstrong, N. R.; Dutta, P.; Marks, T. J. *Chem. Mater.* **2001**, *12*, 15.
(4) Lin, W.; Evans, O. R.; Xiong, R.-G.; Wang, Z. *J. Am. Chem. Soc.* **1998**, *120*, 13272.
(5) Evans, O. R.; Lin, W. *Chem. Mater.* **2001**, *13*, 3009.
(6) Lin, W.; Wang, Z.; Ma, L. *J. Am. Chem. Soc.* **1999**, *121*, 11249.
(7) Halasyamani, P. S.; O'Hare, D. *Chem. Mater.* **1997**, *10*, 66646.
(8) Halasyamani, P. S.; O'Hare, D. *Inorg. Chem.* **1997**, *36*, 6409.
(9) Porter, Y.; Bhuvanesh, N. S. P.; Halasyamani, P. S. *Inorg. Chem.* **2001**, *40*, 1172.
(10) Porter, Y.; Ok, K. M.; Bhuvanesh, N. S. P.; Halasyamani, P. S. *Chem. Mater.* **2001**, *13*, 1910.
(11) Sykora, R. E.; Ok, K. M.; Halasyamani, P. S.; Albrecht-Schmitt, T. E. *J. Am. Chem. Soc.* **2002**, *124*, 1951.
(12) Sykora, R. E.; Ok, K. M.; Halasyamani, P. S.; Wells, D. M.; Albrecht-Schmitt, T. E. *Chem. Mater.* **2002**, *14*, 2741.
(13) Sykora, R. E.; Wells, D. M.; Albrecht-Schmitt, T. E. *Inorg. Chem.* **2002**, *41*, 2697.
(14) Opik, U.; Pryce, M. H. L. *Proc. R. Soc. London* **1937**, *A161*, 220.
(15) Wheeler, R. A.; Whangbo, M. H.; Hughbanks, T.; Hoffman, R.; Burdett, J. K.; Albright, T. A. *J. Am. Chem. Soc.* **1986**, *108*, 2222.
(16) Pearson, R. G. *J. Mol. Struct.* **1983**, *103*, 25.
(17) Kang, S. K.; Tang, H.; Albright, T. A. *J. Am. Chem. Soc.* **1993**, *115*, 1971.
(18) Cohen, R. E. *Nature* **1992**, *358*, 136.

10.1021/ic025992j CCC: $25.00 © 2003 American Chemical Society
Published on Web 12/10/2002

example of this is the perturbation of the Nb(V) centers in $LiNbO_3$ along the C_4 axis of the NbO_6 octahedra. This distortion, which is caused by the symmetry-allowed mixing of a low-lying excited state (LUMO) with the ground state (HOMO), eliminates the center of inversion that would normally be found in an MO_6 octahedron and ultimately leads to the formation of an acentric structure. It should be noted, however, that these distortions are not always directly responsible for large SHG responses, as has been shown in $CsMOB_2O_5$ (M = Nb, Ta), where the boron oxide substructures provide a more significant contribution to the NLO properties than do the distortions of the NbO_6 or TaO_6 octahedra.[23]

Second-order Jahn−Teller distortions also play an important role in the geometries of ions with a nonbonding, but stereochemically active, lone-pair of electrons such as Pb(II), Se(IV), Te(IV), and I(V). The environments around these atoms can be qualitatively understood in terms of the VSEPR model; however, the stereochemical activity of the lone-pair is in fact the result of s−p mixing (HOMO−LUMO interactions) that lowers the energy of the orbital where the lone-pair resides and simultaneously perturbs the geometry around the central atom.[24] The heavier members of groups 16 and 17 are particularly useful examples of this phenomenon because these elements often form air-stable, colorless, and thermally robust oxoanions where the central atom retains a chemically inert lone-pair. The critical feature of these anions is that they have a propensity for aligning in the solid state to form polar solids. Even in the absence of true alignment, these anions will often force structures into noncentrosymmetric architectures because they cannot be placed directly on centers of inversion or higher symmetry. Therefore, anions such as selenite,[25−29] tellurite,[30] and iodate[11,12,31−40] have played important roles in the development of noncentrosymmetric oxides. Recent examples of main group oxides that display alignment of nonbonding electrons include $In_2(Se_2O_5)_3$,[41] Te_2SeO_7,[42] Bi_2TeO_5,[43] and $TeSeO_4$.[44]

The SOJT distortions of both high-valent transition metals and anions containing nonbonding electron pairs can be combined to yield a variety of NCS solids. This concept has been realized in the following families of compounds: $AVSeO_5$ (A = Rb, Cs),[25] $A(VO)_3(SeO_3)_2$ (A = NH_4, K, Rb, Cs),[25,26] $A_2(MoO_3)_3SeO_3$ (A = NH_4, Rb, Cs, Tl),[26−29] $AMoO_3(IO_3)$ (A = Rb, Cs),[11] $A[(VO)_2(IO_3)_3O_2]$ (A = NH_4, Rb, Cs),[12] and $Na_2TeW_2O_9$.[30] The latter three examples have been shown to have large SHG responses from 400 to 500× that of α-quartz.[11,12,30] The goal of combining two different distorted moieties would be to have both of the distortions cooperatively align along a single crystallographic axis. To date, alignment of both types of SOJT distortions in this manner has not been achieved in transition metal compounds.

Another possible hybridization of NCS compounds is to couple optical or magnetic transitions with physical properties derived from the acentricity of the structures. In particular, seminal work at Bell Labs, some three decades ago, demonstrated that transition metal and rare earth iodates that possess d- or f-electrons could be prepared in order to test this hypothesis. Examples of these compounds include $Co(IO_3)_2$,[31] $Cu(IO_3)_2$,[32,33] and $Ln(IO_3)_3 \cdot nH_2O$ ((Ln = Ce−Lu; $n = 0-6$).[34−40] In this present study, we seek to expand upon the early work performed at Bell Labs by combining the electronic transitions derived from f-block elements with the potential for the alignment of both a SOJT distorted transition metal, and a SOJT distorted anion. These compounds take the form of the polar and chiral, rare earth molybdenyl iodates $RE(MoO_2)(IO_3)_4(OH)$ [*RE* = Nd (**1**), Sm (**2**), Eu (**3**)], which have been characterized by X-ray diffraction, vibrational spectroscopy, and second-harmonic generation measurements.

Experimental Section

Syntheses. MoO_3 (99.95%, Alfa-Aesar), I_2O_5 (98%, Alfa-Aesar), HIO_3 (99.5%, Alfa-Aesar), Eu_2O_3 (99.999%, Aldrich Chemical Co.), Sm_2O_3 (99.99%, Alfa-Aesar), and Nd_2O_3 (99.9% Alfa-Aesar) were used as received. $RE(IO_3)_3$ [*RE* = Nd, Sm, Eu] species were prepared by literature methods.[34−40] Distilled and Millipore filtered water with a resistance of 18.2 MΩ was used in all reactions. Reactions were run in Parr 4749 23-mL autoclaves with PTFE liners for 3 days at 200 °C and cooled at a rate of 9 °C/h to 23 °C. The reactions reported produced the highest yields of the desired compounds. SEM/EDX analyses were performed using a JEOL 840/

(19) Burdett, J. K. *Molecular Shapes*; Wiley-Interscience: New York, 1980.
(20) Kunz, M.; Brown, I. D. *J. Solid State Chem.* **1995**, *115*, 395.
(21) Goodenough, J. B.; Longo, J. M. Crystallographic and magnetic properties of perovskite and perovskite-related compounds; In *Landolt-Bornstein*; Hellwege, K. H.; Hellwege, A. M., Eds.; Springer-Verlag: Berlin, 1970; Vol. 4, pp 126−314.
(22) Brown, I. D. *Acta Crystallogr.* **1977**, *B33*, 1305.
(23) Akella, A.; Keszler, D. A. *J. Solid State Chem.* **1995**, *120*, 74.
(24) Halasyamani, P. S.; Poeppelmeier, K. R. *Chem. Mater.* **1998**, *10*, 2753.
(25) Kwon, Y.-U.; Lee, K.-S.; Kim, Y. H. *Inorg. Chem.* **1996**, *35*, 1161.
(26) Vaughey, J. T.; Harrison, W. T. A.; Dussack, L. L.; Jacobson, A. J. *Inorg. Chem.* **1994**, *33*, 4370.
(27) Harrison, W. T. A.; Dussack, L. L.; Jacobson, A. J. *J. Solid State Chem.* **1996**, *125*, 234.
(28) Harrison, W. T. A.; Dussack, L. L.; Jacobson, A. J. *Inorg. Chem.* **1994**, *33*, 6043.
(29) Dussack, L. L.; Harrison, W. T. A.; Jacobson, A. J. *Mater. Res. Bull.* **1996**, *31*, 249.
(30) Ok, K. M.; Halasyamani, P. S. *Chem. Mater.* **2002**, *14*, 3174.
(31) Svenson, C.; Abrahams, S. C.; Bernstein, J. L. *J. Solid State Chem.* **1981**, *36*, 195.
(32) Nassau, K.; Shiever, J. W.; Prescott, B. E. *J. Solid State Chem.* **1973**, *7*, 186.
(33) Nassau, K.; Shiever, J. W.; Prescott, B. E. *J. Solid State Chem.* **1973**, *8*, 260.
(34) Nassau, K.; Shiever, J. W.; Prescott, B. E.; Cooper, A. S. *J. Solid State Chem.* **1974**, *11*, 314.
(35) Liminga, R.; Abrahams, S. C.; Bernstein, J. L. *J. Chem. Phys.* **1975**, *62*, 755.
(36) Nassau, K.; Shiever, J. W.; Prescott, B. E. *J. Solid State Chem.* **1975**, *14*, 122.
(37) Abrahams, S. C.; Bernstein, J. L.; Nassau, K. *J. Solid State Chem.* **1976**, *16*, 173.
(38) Abrahams, S. C.; Bernstein, J. L.; Nassau, K. *J. Solid State Chem.* **1977**, *22*, 243.
(39) Liminga, R.; Abrahams, S. C.; Bernstein, J. L. *J. Chem. Phys.* **1977**, *67*, 1015.
(40) Gupta, P. K. S.; Ammon, H. L.; Abrahams, S. C. *Acta Crystallogr.* **1989**, *C45*, 175.
(41) Ok, K. M.; Halasyamani, P. S. *Chem. Mater.* **2002**, *14*, 2360.
(42) Porter, Y.; Ok, K. M.; Bhuvanesh, N. S. P.; Halasyamani, P. S. *Chem. Mater.* **2001**, *13*, 1910.
(43) Ok, K. M.; Bhuvanesh, N. S. P.; Halasyamani, P. S. *Inorg. Chem.* **2001**, *40*, 1978.
(44) Porter, Y.; Bhuvanesh, N. S. P.; Halasyamani, P. S. *Inorg. Chem.* **2001**, *40*, 1172.

Link Isis instrument. Nd, Sm, Eu, and Mo percentages were calibrated against standards. The reported EDX errors given here are taken from the Isis data and are grossly underestimated by at least an order of magnitude. In general, we have found that EDX ratios are within approximately 4% of the ratios determined from single-crystal X-ray diffraction experiments. IR spectra were collected on a Nicolet 5PC FT-IR spectrometer from KBr pellets.

$Nd(MoO_2)(IO_3)_4(OH)$ (1). MoO_3 (89 mg, 0.616 mmol), I_2O_5 (206 mg, 0.616 mmol), and $Nd(IO_3)_3$ (205 mg, 0.308 mmol) were loaded in a 23-mL PTFE-lined autoclave. Water (1.5 mL) was then added to the solids. The product consisted of pale blue crystals in colorless mother liquor. These crystals become pink under tungsten lighting from a microscope. The mother liquor was decanted from the crystals, which were then washed with water and methanol and allowed to dry. Yield of **1**, 160 mg (53% yield based on Nd). Phase purity was confirmed by powder XRD. No lines were observed that were not also found in the calculated pattern. EDX analysis for **1** provided a Nd/Mo/I ratio of 12.4(3):19.7(3):67.9(3), which is approximately 1:1:4. IR (KBr, cm^{-1}): ν 1066 (ν_{MoOH}, m), 933 (ν_{MoO}, s), 887 (ν_{MoO}, s), 876 (ν_{MoO}, s), 838 (ν_{IO}, m), 821 (ν_{IO}, m), 807 (ν_{IO}, s), 781 (ν_{IO}, s), 767 (ν_{IO}, w), 739 (ν_{IO}, m), 715 (ν_{IO}, s), 662 (ν_{IO}, s, br), 554 (δ_{IO}, s), 453 (δ_{IO}, m), 422 (δ_{IO}, m).

$Sm(MoO_2)(IO_3)_4(OH)$ (2). MoO_3 (71 mg, 0.491 mmol), I_2O_5 (164 mg, 0.491 mmol), and $Sm(IO_3)_3$ (166 mg, 0.245 mmol) were loaded in a 23-mL PTFE-lined autoclave. Water (1.0 mL) was then added to the solids. The product consisted of pale yellow crystals in colorless mother liquor. The mother liquor was decanted from the crystals, which were then washed with water and methanol and allowed to dry. Yield of **2**, 153 mg (62% yield based on Sm). Phase purity was confirmed by powder XRD. No lines were observed that were not also found in the calculated pattern. EDX analysis for **2** provided a Sm/Mo/I ratio of 13.9(4):17.4(4):68.7(4), which is approximately 1:1:4. IR (KBr, cm^{-1}): ν 1056 (ν_{MoOH}, m), 932 (ν_{MoO}, s), 887 (ν_{MoO}, s), 876 (ν_{MoO}, s), 837 (ν_{IO}, m), 820 (ν_{IO}, m), 806 (ν_{IO}, s), 780 (ν_{IO}, s), 762 (ν_{IO}, w), 736 (ν_{IO}, m), 713 (ν_{IO}, s), 664 (ν_{IO}, s, br), 546 (δ_{IO}, s), 458 (δ_{IO}, m), 427 (δ_{IO}, m).

$Eu(MoO_2)(IO_3)_4(OH)$ (3). MoO_3 (71 mg, 0.490 mmol), I_2O_5 (164 mg, 0.490 mmol), and $Eu(IO_3)_3$ (166 mg, 0.245 mmol) were loaded in a 23-mL PTFE-lined autoclave. Water (1.0 mL) was then added to the solids. The product consisted of nearly colorless crystals that fluoresce pink in 365 nm UV light. The mother liquor was decanted from the crystals, which were then washed with water and methanol and allowed to dry. Yield of **3**, 142 mg (57% yield based on Eu). Phase purity was confirmed by powder XRD. No lines were observed that were not also found in the calculated pattern. EDX analysis for **3** provided a Eu/Mo/I ratio of 13.5(4):17.6(4):68.9(4), which is approximately 1:1:4. IR (KBr, cm^{-1}): ν 1049 (ν_{MoOH}, m), 930 (ν_{MoO}, s), 887 (ν_{MoO}, s), 876 (ν_{MoO}, s), 836 (ν_{IO}, m), 819 (ν_{IO}, m), 804 (ν_{IO}, s), 780 (ν_{IO}, s), 760 (ν_{IO}, w), 734 (ν_{IO}, m), 712 (ν_{IO}, s), 658 (ν_{IO}, s, br), 546 (δ_{IO}, s), 459 (δ_{IO}, m), 428 (δ_{IO}, m).

Secord-Order NLO Measurements. Powder SHG measurements were performed on a modified Kurtz-NLO system using a 1064 nm light source.[45] A detailed description of the apparatus has been published.[46] Polycrystalline $Nd(MoO_2)(IO_3)_4(OH)$ (**1**) was ground and sieved into distinct particle size ranges, <20, 20−45, 45−63, 63−75, 75−90, and 90−125 μm. To make relevant comparisons with known SHG materials, crystalline SiO_2 and $LiNbO_3$ were also ground and sieved into the same particle size range. All of the powders were placed in separate capillary tubes. No index-matching fluid was used in any of the experiments. $I^{2\omega}/I^{2\omega}$ (SiO_2) is taken for a particle size range of 45−63 μm.

Table 1. Crystallographic Data for $Nd(MoO_2)(IO_3)_4(OH)$ (**1**), $Sm(MoO_2)(IO_3)_4(OH)$ (**2**), $Eu(MoO_2)(IO_3)_4(OH)$ (**3**)

	Nd-**1**	Sm-**2**	Eu-**3**
formula mass (amu)	988.78	994.89	996.50
color and habit	pale blue prism	yellow prism	colorless prism
cryst syst	monoclinic	monoclinic	monoclinic
space group	$P2_1$ (No. 4)	$P2_1$ (No. 4)	$P2_1$ (No. 4)
a (Å)	6.9383(5)	6.9243(6)	6.9169(6)
b (Å)	14.0279(9)	13.963(1)	13.943(1)
c (Å)	7.0397(5)	7.0229(6)	7.0170(6)
β (deg)	114.890(1)	114.681(1)	114.542(1)
V (Å^3)	621.53(7)	616.99(9)	615.62(9)
Z	2	2	2
T (°C)	−80	−80	−80
λ (Å)	0.71073	0.71073	0.71073
$2\theta_{max}$	56.58	56.61	56.58
ρ_{calcd} (g cm^{-3})	5.278	5.350	5.370
μ(Mo Kα) (cm^{-1})	151.59	158.21	161.8
$R(F)$ for $F_o^2 > 2\sigma(F_o^2)^a$	0.0235	0.0150	0.0223
$R_w(F_o^2)^b$	0.0502	0.0330	0.0399

^{a} $R(F) = \sum||F_o| - |F_c||/\sum|F_o|$. ^{b} $R_w(F_o^2) = [\sum[w(F_o^2 - F_c^2)^2]/\sum wF_o^4]^{1/2}$.

Crystallographic Studies. Crystals of $Nd(MoO_2)(IO_3)_4(OH)$ (**1**), $Sm(MoO_2)(IO_3)_4(OH)$ (**2**), and $Eu(MoO_2)(IO_3)_4(OH)$ (**3**) were mounted on glass fibers with epoxy and aligned on a Bruker SMART APEX CCD X-ray diffractometer. Intensity measurements were performed using graphite monochromated Mo Kα radiation from a sealed tube with a monocapillary collimator. SMART was used for preliminary determination of the cell constants and data collection control. For all compounds, the intensities of reflections of a sphere were collected by a combination of 3 sets of exposures (frames). Each set had a different ϕ angle for the crystal, and each exposure covered a range of 0.3° in ω. A total of 1800 frames were collected with an exposure time per frame of 30 s.

For **1**−**3**, determinations of integral intensities and global cell refinement were performed with the Bruker SAINT (v 6.02) software package using a narrow-frame integration algorithm. These data were subsequently treated with a semiempirical absorption correction using SADABS.[47] Unfortunately, crystals of **1**−**3** grow as irregularly shaped prisms making reliable assignment of the faces tenuous at best. Single crystals of **1** were too small to accurately measure. Therefore, no analytical corrections were applied. However, the thermal parameters for all atoms after correction using SADABS are reasonable. The program suite SHELXTL (v 5.1) was used for space group determination (XPREP), direct methods structure solution (XS), and least-squares refinement (XL).[48] The final refinements included anisotropic displacement parameters for all atoms and a secondary extinction parameter. Some crystallographic details are listed in Table 1. Additional details can be found in Supporting Information.

Results and Discussion

Syntheses. The preparation of $RE(MoO_2)(IO_3)_4(OH)$ [*RE* = Nd (**1**), Sm (**2**), Eu (**3**)] is surprisingly straightforward

(45) Kurtz, S. K.; Perry, T. T. *J. Appl. Phys.* **1968**, *39*, 3798.
(46) Porter, Y.; Ok, K. M.; Bhuvanesh, N. S. P.; Halasyamani, P. S. *Chem. Mater.* **2001**, *13*, 1910.
(47) *SADABS*. Program for absorption correction using SMART CCD based on the method of Blessing: Blessing, R. H. *Acta Crystallogr.* **1995**, *A51*, 33.
(48) Sheldrick, G. M. *SHELXTL PC*, Version 5.0; An Integrated System for Solving, Refining, and Displaying Crystal Structures from Diffraction Data; Siemens Analytical X-ray Instruments, Inc.: Madison, WI, 1994.

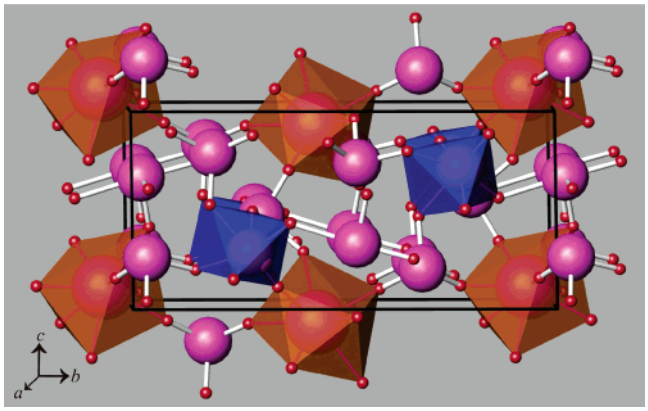

Figure 1. View of the polar and chiral structure of $Sm(MoO_2)(IO_3)_4(OH)$ (**2**). The Sm^{3+} cations are located in eight-coordinate, square antiprismatic environments (orange polyhedra) that are bridged by iodate anions to distorted octahedral MoO_6 units (blue polyhedra). The iodine atoms are shown in purple and the oxygen atoms in red.

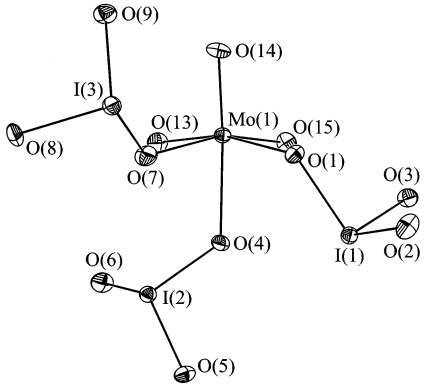

Figure 2. Depiction of the distorted octahedral environment around Mo(1). The Mo(VI) centers are bound by two terminal oxo atoms in a *cis* geometry, three bridging iodate anions in a *fac* arrangement, and a hydroxo group. A second-order Jahn−Teller distortion shifts the Mo atom 0.362 Å away from the center of an idealized MoO_6 octahedron. This particular distortion is between a C_3 and C_2 axis.

and can be achieved by reacting $RE(IO_3)_3$ [*RE* = Nd, Sm, Eu] with I_2O_5 and MoO_3 in a 1:2:2 molar ratio at 200 °C for 3 days in aqueous media under autogenously generated pressure. Other molar ratios also produce **1**−**3**, and the region of stability for these phases appears to be quite wide; however, unreacted $RE(IO_3)_3$ and $RE(IO_3)_3 \cdot nH_2O$ (n = 1, 2) were typically found in the product mixtures at other stoichiometries. In addition, these preparations have been preformed from 180 to 200 °C and with durations of 3−5 days without significant effect on product yield or crystal size. These compounds are isolated in the form of crystalline solids with the coloration being dependent on the lanthanide employed. In all cases, the crystals are quite small, and no single crystals larger than 0.3 mm were isolated for these reactions. All crystals have irregular prismatic habits.

Crystals of **1** are pale blue but appear pink when irradiated with tungsten light from a microscope. The crystals revert to pale blue once removed from irradiation by the tungsten light. Compound **2** forms pale yellow crystals. Crystals of **3** are nearly colorless under ambient light but emit strong pink luminescence when irradiated with 365 nm hand-held UV light. The emission spectra from single crystals of **1**−**3** were measured using a fluorescence microscope. All compounds show emission lines expected from the specific lanthanide in the compound. The emission from **2** is not visible to the naked eye.

Structures. $RE(MoO_2)(IO_3)_4(OH)$ [*RE* = Nd (1), Sm (2), Eu (3)]. The structures of **1**−**3** are complex, polar, and chiral, three-dimensional networks composed of eight-coordinate, square antiprismatic RE^{3+} cations, distorted octahedral Mo(VI) centers, and bridging iodate anions. A view of the complex unit cell of **1**−**3** is shown in Figure 1. This structure will be broken down into distinct substructures for the sake of a coherent discussion, although it should be noted that there are no true features of lower dimensionality present. Furthermore, all bond distances and angles will be derived from the structure of **2** for simplicity.

To begin with, the Mo(VI) ions are ligated by two, terminal oxo atoms in a *cis* geometry. This is the classical molybdenyl unit defined by two short Mo═O distances of 1.718(4) and 1.726(4) Å. Three additional positions are occupied by bridging iodate anions with Mo−O(IO_3) distances of 2.157(4), 2.165(4), and 2.148(4) Å. The final coordination site is filled with a hydroxo group with Mo−OH distance of 1.823(4) Å. The hydroxyl hydrogen atom was indeed located by performing a Fourier synthesis on the low-angle X-ray data, but this atom has been excluded from the structure refinement because of the large electron density of other atoms in the structure. The Mo−OH stretching mode was also clearly observed in the IR spectrum at 1056 cm^{-1}.[49] Mo(VI) is highly susceptible to a second-order Jahn−Teller distortion and is located 0.362 Å away from the center of an idealized MoO_6 octahedron. This particular distortion is between a C_3 and C_2 axis of the octahedron. This is an atypical environment for Mo(VI) because it is normally orthorhombically distorted along a C_2 axis yielding a 2 + 2 + 2 bonding scheme with two long, two intermediate, and two short bonds.[11,26−29] The distorted MoO_6 octahedron from **2** is depicted in Figure 2.

The square antiprismatic coordination environment of the RE^{3+} cations is formed by interactions with seven bridging iodate anions with bond distances ranging from 2.378(4) to 2.469(4) Å. The eighth site is formed with a rather short interaction between the oxygen atom from the molybdenyl unit and the rare earth cation, with a Sm−O distance of 2.456(4) Å, which compares well with the Sm−O(IO_3) distances. The local environment around Sm(1) in **2** is shown in Figure 3. It is interesting to note that only a single iodate anion bridges between each Sm and Mo atom.

There are four crystallographically unique iodate anions in this structure. Three of these anions bridge between two Sm(III) ions and one Mo(VI) atom. These I(V) centers show normal I═O bond distances ranging from 1.792(4) to 1.843(3) Å. The fourth iodate anion, containing I(4), shows some unusual features for an iodate compound. First, this iodate anion is actually present in the form of an IO_{3+1} polyhedron where there are two short I═O bond distances

(49) Nakamoto, K. *Infrared and Raman Spectra of Inorganic and Coordination Compounds*, 5th ed.; Wiley-Interscience: New York, 1997.

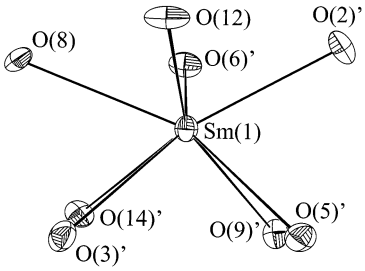

Figure 3. Illustration of the eight-coordinate, square antiprismatic environment around Sm(1) in **2**.

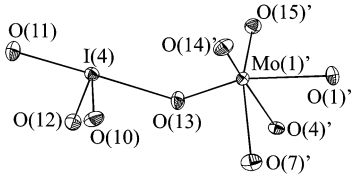

Figure 4. IO_{3+1} distorted square pyramid containing I(4). Here, there are two short I═O bond distances of 1.789(4) Å to O(10) and O(12), one intermediate distance of 1.951(4) Å to O(11), and one long distance of 2.285(4) Å to O(13).

of 1.789(4)Å, one intermediate distance of 1.951(4) Å, and one long distance of 2.285(4) Å. An illustration of this anion is shown in Figure 4. While IO_{3+1} polyhedra are common in iodate compounds,[50−52] the fourth interaction is usually on the order of 2.5 Å. Furthermore, this interaction is most typically formed between two iodate anions.

The only iodine oxide compounds that we have identified that show similar structural features with **1**−**3** are those containing the iodyl cation, $[I_2O_4]^{2+}$.[53−55] In **1**−**3**, this contact is actually occurring between the hydroxo group bound to the Mo(VI) center and an iodate anion that does not coordinate the same metal atom. This is similar to the interaction between the iodyl cation and the disulfate anion in $(IO_2)_2S_2O_7$.[53−55] The long I···O interaction found in **1**−**3** is approximately 0.2 Å shorter than expected from IO_3^{1-}···IO_3^{1-} dimerization. The I═O bond *trans* to this interaction shows substantial lengthening from an expected distance of approximately 1.8 to 1.951(4) Å. Despite the added I···O interaction, the lengthening of the *trans* I−O bond allows for the maintenance of the formally +5 oxidation state as indicated by the bond valence sum of 5.14.[56,57] The geometry and bond distances for this IO_{3+1} unit, which occur in the form of a distorted square pyramid, are quite similar to those found for the TeO_{3+1} polyhedra in α-$Tl_2[UO_2(TeO_3)_2]$.[58] Substantial geometric distortions in Te(IV) oxoanions as the result of long Te···O interactions are in fact well represented.[58−62]

Table 2. Selected Bond Distances (Å) and Angles (deg) for $Sm(MoO_2)(IO_3)_4(OH)$ (**2**)

Sm(1)−O(2)′(#1)[a]	2.378(4)	I(1)−O(1)	1.840(4)
Sm(1)−O(3)′(#2)[a]	2.463(4)	I(1)−O(2)	1.795(4)
Sm(1)−O(5)′(#3)[a]	2.382(4)	I(1)−O(3)	1.816(3)
Sm(1)−O(6)′(#4)[a]	2.344(4)	I(2)−O(4)	1.843(3)
Sm(1)−O(8)	2.442(4)	I(2)−O(5)	1.795(4)
Sm(1)−O(9)′(#5)[a]	2.465(4)	I(2)−O(6)	1.798(4)
Sm(1)−O(12)	2.469(4)	I(3)−O(7)	1.828(4)
Sm(1)−O(14)′(#5)[a]	2.456(4)	I(3)−O(8)	1.792(4)
Mo(1)−O(1)	2.148(4)	I(3)−O(9)	1.795(4)
Mo(1)−O(4)	2.157(4)	I(4)−O(10)	1.789(4)
Mo(1)−O(7)	2.165(4)	I(4)−O(11)	1.951(4)
Mo(1)−O(13) (OH)	1.823(4)	I(4)−O(12)	1.789(4)
Mo(1)−O(14) (Mo═O)	1.718(4)	I(4)−O(13)′(#4)[a]	2.285(4)
Mo(1)−O(15) (Mo═O)	1.726(4)		

Bond Angles (deg) for the IO_{3+1} Distorted Square Pyramid

O(10)−I(4)−O(11)	91.46(18)	O(11)−I(4)−O(12)	93.03(17)
O(10)−I(4)−O(12)	99.81(17)	O(11)−I(4)−O(13)	178.58(16)
O(10)−I(4)−O(13)	88.85(16)	O(12)−I(4)−O(13)	85.55(16)

[a] (#1) $-x+2, y-1/2, -z+2$; (#2) $-x+3, y-1/2, -z+2$; (#3) $-x+3, y-1/2, -z+3$; (#4) $x-1, y, z$; (#5) $x, y, z+1$.

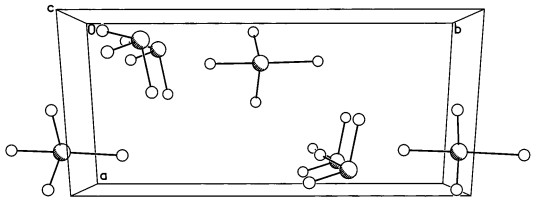

Figure 5. Iodate anions containing I(3) and I(4) show cooperative alignment of their stereochemically active lone-pairs of electrons along the polar *b*-axis in $Nd(MoO_2)(IO_3)_4(OH)$ (**1**), $Sm(MoO_2)(IO_3)_4(OH)$ (**2**), and $Eu(MoO_2)(IO_3)_4(OH)$ (**3**).

Therefore, the structures of **1**−**3** represent important links between iodate and tellurite chemistry. Selected bond distances and angles from **2** are given in Table 2. Similar distances and angles for **1**−**3** can be found in the Supporting Information as CIF data.

Structure−Property Relationships. The polar and chiral space group $P2_1$ indicates a specific direction of polarization along the *b*-axis for **1**−**3**. Examination of the directionality of the four independent iodate anions and the distorted MoO_6 octahedron indicates that two iodate anions containing I(3) and I(4) show net alignment along the *b*-axis as demonstrated by Figure 5. The significant degree of polarization of the I−O bond might lead to a large second-harmonic generation response, and such measurements also help to confirm the assignment of this structure in a noncentrosymmetric setting. SHG measurements were performed using a modified Kurtz-NLO system with a 1064 nm light source on powders ground from crystals of **1**. These measurements should also be representative of the SHG properties of **2** and **3**. Generation of SHG light of 532 nm was carefully measured, and these studies indicated a reasonably large response for **1** of 350× that of α-quartz. The birefringence of **1** is significant enough for phase-matchability (type 1) as shown in Figure 6.

(50) Bean, A. C.; Peper, S. M.; Albrecht-Schmitt, T. E. *Chem. Mater.* **2001**, *13*, 1266.
(51) Bean, A. C.; Ruf, M.; Albrecht-Schmitt, T. E. *Inorg. Chem.* **2001**, *40*, 3959.
(52) Bean, A. C.; Albrecht-Schmitt, T. E. *J. Solid State Chem.* **2001**, *161*, 416.
(53) Jansen, M.; Kraft, T. *Chem. Ber.* **1997**, *130*, 307.
(54) Jansen, M.; Müller, R. *Angew. Chem., Int. Ed. Engl.* **1997**, *36*, 255.
(55) Jansen, M.; Müller, R. *Z. Anorg. Allg. Chem.* **1997**, *623*, 1055.
(56) Brown, I. D.; Altermatt, D. *Acta Crystallogr.* **1985**, *B41*, 244.
(57) Brese, N. E.; O'Keeffe, M. *Acta Crystallogr.* **1991**, *B47*, 192.
(58) Almond, P. M.; McKee, M. L.; Albrecht-Schmitt, T. E. *Angew. Chem., Int. Ed.* **2002**, *114*, 3576.
(59) Johnston, M. G.; Harrison, W. T. A. *J. Am. Chem. Soc.* **2002**, *124*, 4576.
(60) Dutrielh, M.; Thomas, P.; Champarnaud-Mesjard, J. C.; Frit, B. *Solid State Sci.* **2001**, *3*, 423.
(61) Feger, C. R.; Kolis, J. W. *Inorg. Chem.* **1998**, *37*, 4046.
(62) Feger, C. R.; Schimek, G. L.; Kolis, J. W. *J. Solid State Chem.* **1999**, *143*, 246.

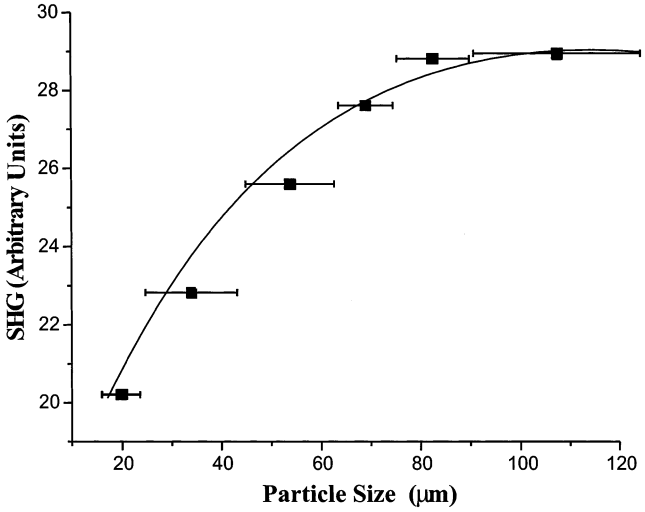

Figure 6. Phase matching curve (type 1) for $Nd(MoO_2)(IO_3)_4(OH)$ (**1**). The curve is to guide the eye and is not a fit to the data.

Calculations using methods described earlier[10,63] give an average NLO susceptibility, $\langle d_{ijk}^{2\omega} \rangle$ or $\langle d_{eff} \rangle$, of 21 pm/V.

Conclusions

This present study demonstrates that rare earth iodates containing second-order Jahn−Teller distorted transition metals can indeed be prepared in reasonable yield. The structures of these compounds were determined to be both polar and chiral and, therefore, exhibit frequency-doubling characteristics as shown via SHG measurements. Future studies will address the structure−property relationships in other rare earth transition metal iodates with the goal of finding cooperative SOJT distortions in both the iodate anions and the transition metals.

Acknowledgment. T.E.A.-S. acknowledges NASA (ASGC) and the Department of Energy, Heavy Elements Program (Grant DE-FG02-01ER15187) for partial support of this work. P.S.H. acknowledges the Robert A. Welch Foundation for support. P.S.H. also acknowledges support from the NSF-Career Program through DMR-0092054. An acknowledgment is made to the donors of the Petroleum Research Fund, administered by the American Chemical Society, for partial support of this research (T.E.A.-S. and P.S.H.). P.S.H. is a Beckman Young Investigator.

Supporting Information Available: X-ray crystallographic files for $NdMoO_2(IO_3)_4(OH)$ (**1**), $SmMoO_2(IO_3)_4(OH)$ (**2**), $EuMoO_2(IO_3)_4(OH)$ (**3**) in CIF format. This material is available free of charge via the Internet at http://pubs.acs.org.

IC025992J

(63) Ok, K. M.; Bhuvanesh, N. S. P.; Halasyamani, P. S. *J. Solid State Chem.* **2001**, *161*, 57.